Development of a Highly Efficient and Accurate Wind-Wave Simulation Framework for Operational Data Assimilation

Lian Shen
Department of Civil Engineering
Johns Hopkins University
Baltimore, MD 21218
phone: (410) 516-5033 fax: (410) 516-7473 email: LianShen@jhu.edu

Award Number: N00014-09-1-0395

LONG-TERM GOAL

This research aims at developing a highly efficient yet accurate computation framework for simulation and prediction of wave and wind coupled motions with wave phases being resolved, which will lead to an advanced data assimilation tool to provide more comprehensive environmental input for naval applications. Our ultimate goal is to pave the way for developing an operational tool for the Navy to use for ocean-wave-atmosphere battlespace sensing and prediction with high resolution.

OBJECTIVES

The scientific and technical objectives of this research are to:

(1) use the detailed physics revealed in coupled wind-wave simulations to obtain a fundamental understanding of wave surface layer processes, based on which physics-based advanced wave-layer models can be developed;

(2) adopt a highly accurate immersed boundary method to perform turbulence-wave simulation on fixed Cartesian grid to achieve superior computation efficiency; and

(3) use the developments in (1) and (2) to pave the way for the development of a computation framework for data assimilation with a focus on the reconstruction of wavefield and the retrieval of coherent flow structures from field measurements.

APPROACH

This research builds on the combined simulation of wind-wave interaction achieved in a fully dynamical, two-way coupled context. In the simulation, evolution of wavefield is simulated with an efficacious high-order spectral (HOS) method that captures all of the dynamically important nonlinear wave interaction processes. Large-eddy simulation (LES) is performed for the marine atmospheric boundary layer (MABL) in a direct, physical context with wave phases of the broadband wavefield being resolved. In LES, fully resolving the boundary layer at the air-sea interface is prohibitively expensive. We use a wall-layer model to represent the momentum exchange between the outer layer

Report Documentation Page

Form Approved
OMB No. 0704-0188

1. REPORT DATE	2. REPORT TYPE	3. DATES COVERED
30 SEP 2009	**Annual**	**00-00-2009 to 00-00-2009**

4. TITLE AND SUBTITLE	5a. CONTRACT NUMBER
Development Of A Highly Efficient And Accurate Wind-Wave Simulation Framework For Operational Data Assimilation	5b. GRANT NUMBER
	5c. PROGRAM ELEMENT NUMBER
6. AUTHOR(S)	5d. PROJECT NUMBER
	5e. TASK NUMBER
	5f. WORK UNIT NUMBER
7. PERFORMING ORGANIZATION NAME(S) AND ADDRESS(ES) **Johns Hopkins University,Department of Civil Engineering,Baltimore,MD,21218**	8. PERFORMING ORGANIZATION REPORT NUMBER
9. SPONSORING/MONITORING AGENCY NAME(S) AND ADDRESS(ES)	10. SPONSOR/MONITOR'S ACRONYM(S)
	11. SPONSOR/MONITOR'S REPORT NUMBER(S)

12. DISTRIBUTION/AVAILABILITY STATEMENT
Approved for public release; distribution unlimited

13. SUPPLEMENTARY NOTES
Code 1 only

14. ABSTRACT
This research aims at developing a highly efficient yet accurate computation framework for simulation and prediction of wave and wind coupled motions with wave phases being resolved, which will lead to an advanced data assimilation tool to provide more comprehensive environmental input for naval applications. Our ultimate goal is to pave the way for developing an operational tool for the Navy to use for ocean-wave-atmosphere battlespace sensing and prediction with high resolution.

15. SUBJECT TERMS

16. SECURITY CLASSIFICATION OF:			17. LIMITATION OF ABSTRACT	18. NUMBER OF PAGES	19a. NAME OF RESPONSIBLE PERSON
a. REPORT	b. ABSTRACT	c. THIS PAGE			
unclassified	**unclassified**	**unclassified**	**Same as Report (SAR)**	**9**	

and the small but dynamically important eddies in the inner layer. The extensive, high resolution data obtained from the coupled LES-HOS simulation provide a unique opportunity to develop, assess, and calibrate wave-layer models.

In this study, we will adopt the immersed boundary method (IBM) approach for turbulence simulation near surface waves, with the constraints of the moving water surface represented by a body force through a discrete force method, which can capture the boundary precisely. We use large-scale high-performance computation on massively parallel computers. Our coupled LES-HOS code is parallelized using massage passing interface (MPI) based on domain decomposition. With the developments of wave-layer model and IBM method for turbulence-wave interaction, the computational cost will be reduced significantly. The simulation capabilities developed in this study will be used for data assimilation with a focus on the retrieval of coherent flow structures and the reconstruction of wavefield based on measurements. The simulation results obtained in this study will be compared with and validated against field measurement data.

WORK COMPLETED

This project started during the fiscal year of 2009. During this first phase of the project, substantial progresses have been made, which include:

- Establishment of the computation framework for the mechanistic investigation of wind-wave interactions and for the development of efficient modeling approaches
- Comparison and validation of simulation results with measurement and simulation data in the literature
- Elucidation of the fundamental physics of wind turbulence over water waves through analysis of turbulent kinetic energy budget, wave drag, and Reynolds stress
- Characterization of unique vortical structures over waves, and elucidation of the important role of coherent vortices play in wind-wave momentum transfer
- Analysis of quadrants contribution to Reynolds stress and the correlation with coherent vertical structures, which establishes a physical basis for the development of wave-layer models for efficacious simulation

RESULTS

The development of advanced wave-layer model for wind turbulence simulation requires a deep understanding of the mechanisms of wind-wave interaction. Based on our simulation data, we investigated the fundamentals of the turbulence dynamics. Figure 1 shows the mean profiles of the budget terms of the turbulent kinetic energy for winds over water waves with ak=0.25 and c/u*=2, 14, and 25. For all of the cases, production and dissipation terms dominate except near the surface where the production term becomes zero and the viscous diffusion term balances the dissipation term. For c/u*=2, the peak of production term is located around z^+=25, while for c/u*=14 and 25, the production peaks move towards the surface to around z^+=10.

The wind turbulence exchanges momentum and energy with the ocean through the drag force at the sea surface. The total drag acting on the sea surface, F_{total}, consists of several components. One important

component, the wave-induced drag F_{wave}, represents the momentum exchange between the wind turbulence and the water wave. Figure 2 shows the ratio F_{wave}/ F_{total} as a function of wave steepness ak for the slow wave case. Our simulation result shows that as ak increases, F_{wave}/ F_{total} increases as well, indicating the enhanced momentum exchange between wind and wave for large wave steepness. The comparison shown in figure 2 indicates our simulation result agrees very well with existing measurements and the theoretical prediction by Belcher (1999) (see equation 15 in Peirson & Garcia 2008).

The distribution of Reynolds stress is highly dependent on the wave phase, and the dependence varies as the wave age changes. The Reynolds stress can be decomposed into contributions from four quadrants: Q1 (u'>0, w'>0), Q2 (u'<0, w'>0), Q3 (u'<0, w'<0), and Q4 (u'>0, w'<0). Figure 3 shows the decomposed Reynolds stress distributions over a slow water wave with (ak, c/u*) = (0.25, 2). It is apparent that for this slow wave case, the Q2 and Q4 events are responsible for most of the Reynolds stress, while the contributions from Q1 and Q3 are much smaller. In figure 3(b), the high intensity region of Reynolds stress due to Q2 (ejection) starts above the wave trough, extends to the downstream direction, lifts up above the wave crest, and then becomes weak further downstream. In figure 3(d), the high intensity region of Reynolds stress due to Q4 (sweep) is found to be located right above the wave trough.

Figure 4 shows the distributions of the decomposed Reynolds stress over a fast wave with (ak, c/u*) = (0.25, 25), which is found to be quite different from those above the slow wave as shown in figure 3. For this fast wave case, the Q1 and Q3 events produce negative Reynolds stress on the windward side of the wave crest, while the Q2 and Q4 events contribute to positive Reynolds stress on the leeward side of the wave crest.

Figure 5 shows the effect of turbulence motion on the wave surface shear stress. Similar to the flat wall boundary layer case, the vertical motions induced by the quasi-streamwise vortices greatly enhance the vertical momentum transport and thus the friction drag. Here we show the intermediate wave case (c/u* = 14) as an example. Figure 5(a) shows the surface shear stress distribution in the conditionally averaged flow field associated with the Q1 (u'>0, w'>0) motion above the windward face of the wave crest. The vortical structure associated with Q1 motion is found to consist of a counter-rotating vortex pair, which has a considerable vertical component near the upstream end. The positive streamwise velocity fluctuation associated with the vertical component of the vortex pair enhances the streamwise velocity in between, and causes 10% to 15% increase of surface shear stress on the windward face. Figure 5(b) shows the surface shear stress distribution in the conditionally averaged flow field associated with the Q4 (u'>0, w'<0) motion above the leeward face of the wave crest. The vortical structure associated with Q4 motion is found to consist of a counter-rotating streamwise vortex pair. The downwelling motion associated with the horizontal vortex pair sweeps the high speed fluid towards the wave surface, and causes 10% to 20% increase of shear stress on the leeward face. Such information is essential for the development of physics-based models for efficacious wind-wave simulation proposed in this study.

IMPACT/APPLICATION

This project addresses the basic physics of wave surface layer, which will lead to better understanding of turbulence-wave interaction dynamics. It is expected to improve simulation efficiency significantly, which will lead to a powerful computational capability for direct comparison between measurement and modeling and for data fusion in field experiments.

REFERENCES

Banner, M. L. 1990 “The influence of wave breaking on the surface pressure distribution in wind-wave interactions,” *J. Fluid Mech.* **211**, 463-495.

Banner, M. L. & Peirson, W. L. 1998 “Tangential stress beneath wind-driven air-water interface,” *J. Fluid Mech.* **364**, 115-145.

Belcher, S. E. 1999 “Wave growth by non-separated sheltering,” *Eur. J. Mech.* B/*Fluids* **18**, 447-462.

Bole, J. B. 1967 “Response of gravity water waves to wind excitation,” PhD thesis, Dept. of Civil Engineering, Stanford University.

Mastenbroek, C., Makin, V. K., Garat, M. H. & Giovanangeli, J. P. 1996 “Experimental evidence of the rapid distortion of turbulence in the air flow over water waves,” *J. Fluid Mech.* **318**, 273-302.

Mastenbroek, C. 1996 “Wind-wave interaction,” PhD thesis, Delft Tech. Univ.

Peirson, W. & Garcia, A. W. 2008 “On the wind-induced growth of slow water waves of finite steepness,” *J. Fluid Mech.* **608**, 243-274.

HONORS/AWARDS/PRIZES

T. F. Ogilvie Young Investigator Lectureship
Keynote speaker at the 2nd International Conference on Turbulence and Interaction

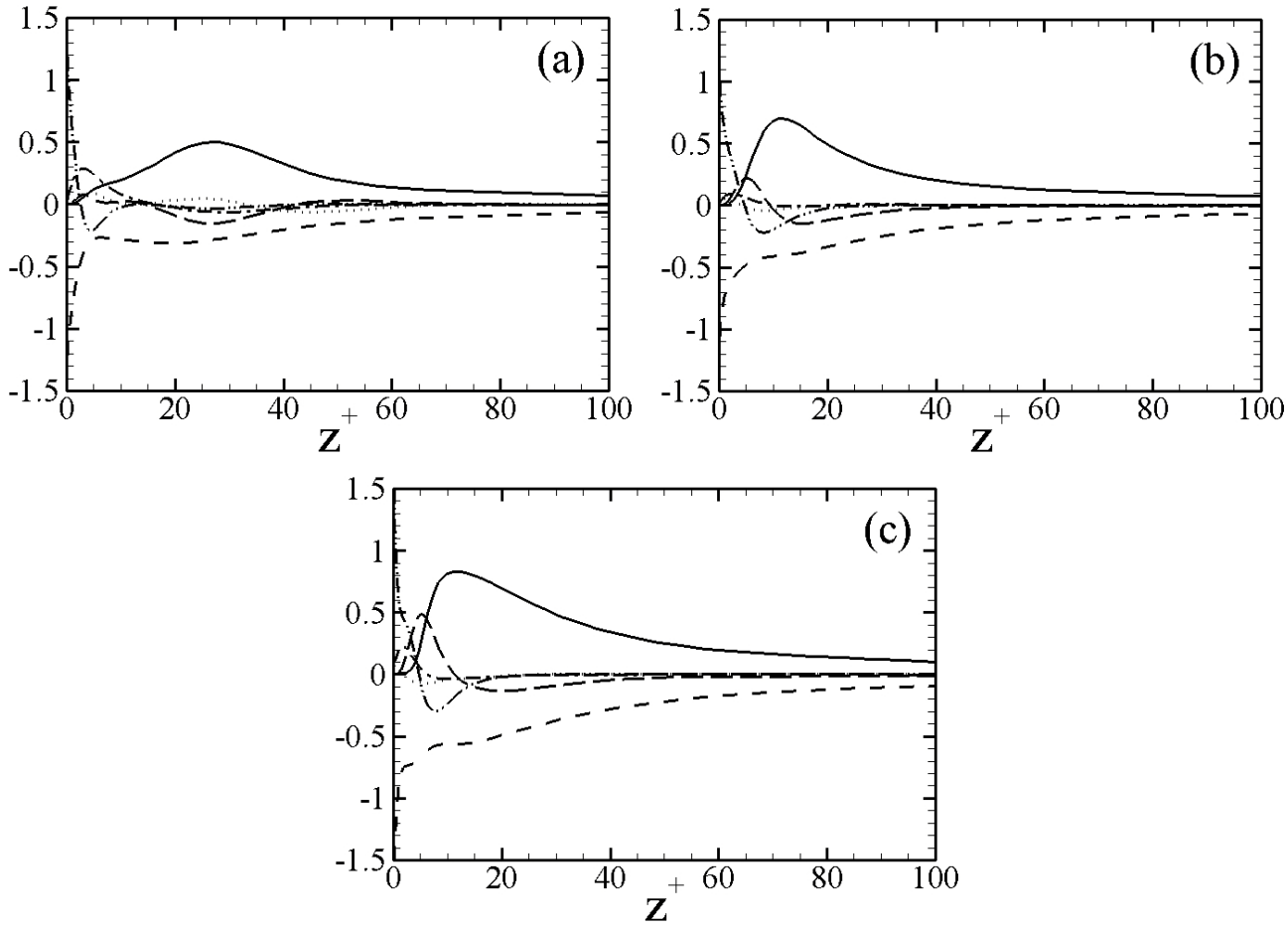

Figure 1. Budget of turbulent kinetic energy in wind over water waves with steepness ak=0.25 and wave ages: (a) c/u*=2; (b) c/u*=14; and (c) c/u*=25. Line patterns for budget terms: dotted line, advection; solid line, production; dash-dot line, pressure transport; dash-dot-dot line, viscous diffusion; long dashed line, turbulent transport; dashed line, dissipation. All terms are normalized by $100u^{*3}/\lambda$.

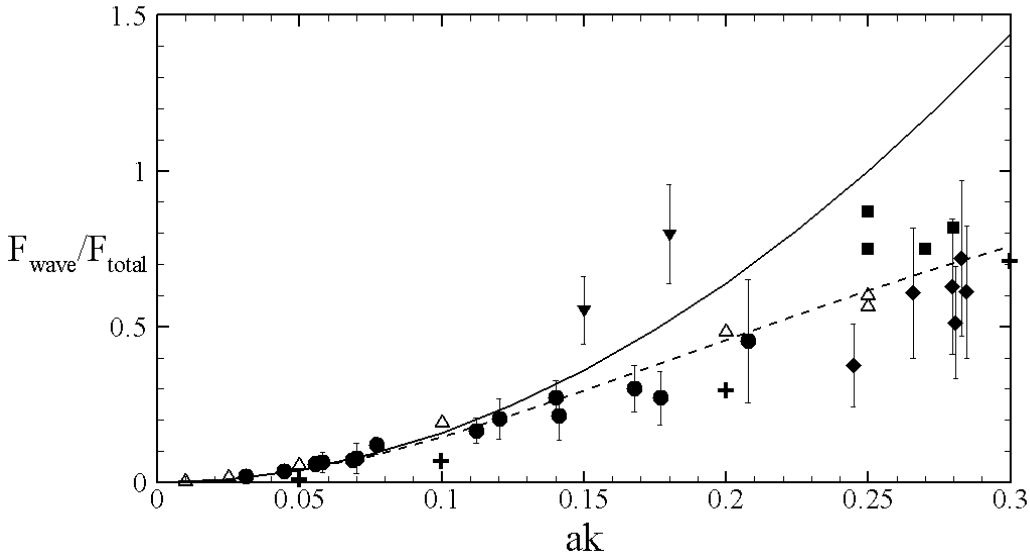

Figure 2. Ratio of wave drag to total surface drag plotted as a function of wave steepness. Measurement data compiled by Peirson & Garcia (2008) are denoted by solid symbols with error bars: ▲, Bole (1967); ■, Banner (1990); ▼, Mastenbroek et al. (1996); ◆, Banner & Peirson (1998); and ●, Peirson & Garcia (2008). LRR turbulence closure results by Mastenbroek (1996) are denoted by +. Results of the present study are denoted by △.

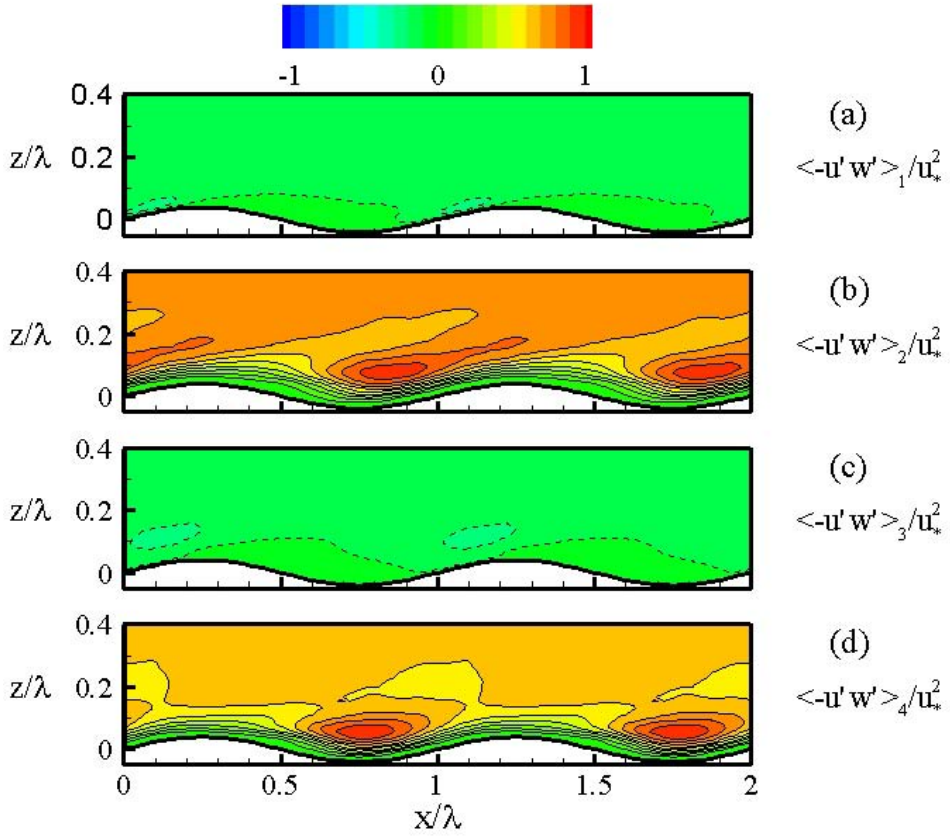

Figure 3. For wind over water wave with (ak, c/u*) = (0.25, 2), contributions to Reynolds stress from quadrants: (a) Q1 (u'>0, w'>0); (b) Q2 (u'<0, w'>0); (c) Q3 (u'<0, w'<0); and (d) Q4 (u'>0, w'<0). Dashed contour lines represent negative values. The contour interval is 0.1. The surface wave propagates in the +x-direction.

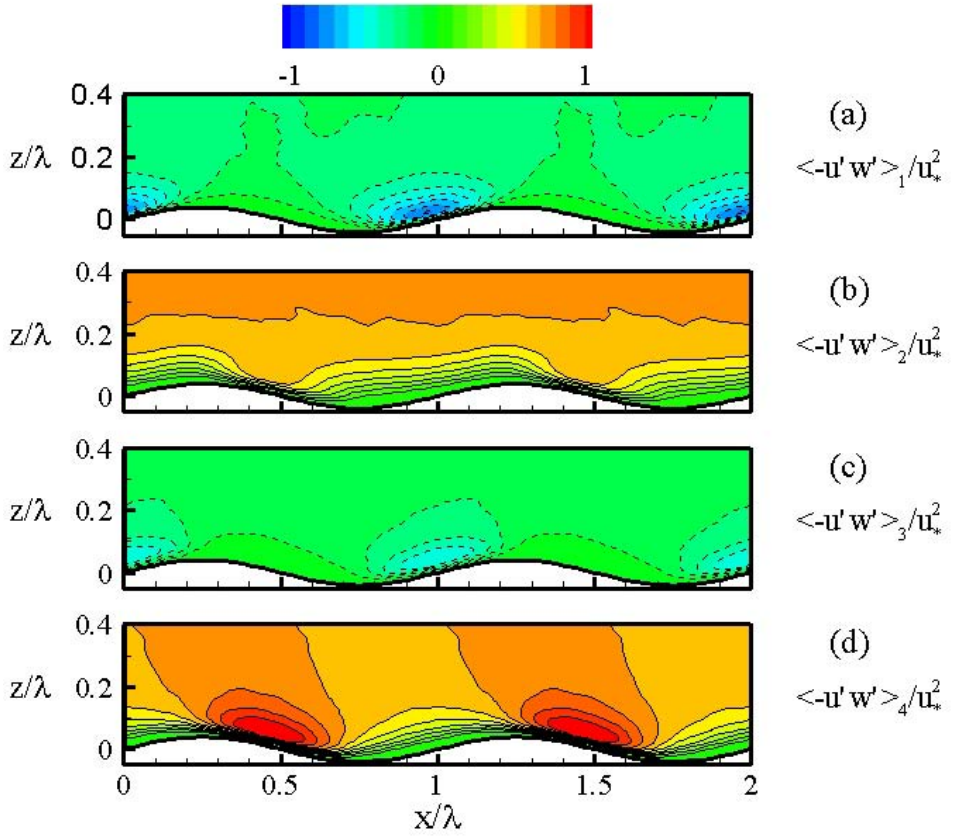

Figure 4. For wind over water wave with (ak, c/u*) = (0.25, 25), contributions to Reynolds stress from quadrants: (a) Q1 (u'>0, w'>0); (b) Q2 (u'<0, w'>0); (c) Q3 (u'<0, w'<0); and (d) Q4 (u'>0, w'<0). Dashed contour lines represent negative values. The contour interval is 0.1. The surface wave propagates in the +x-direction.

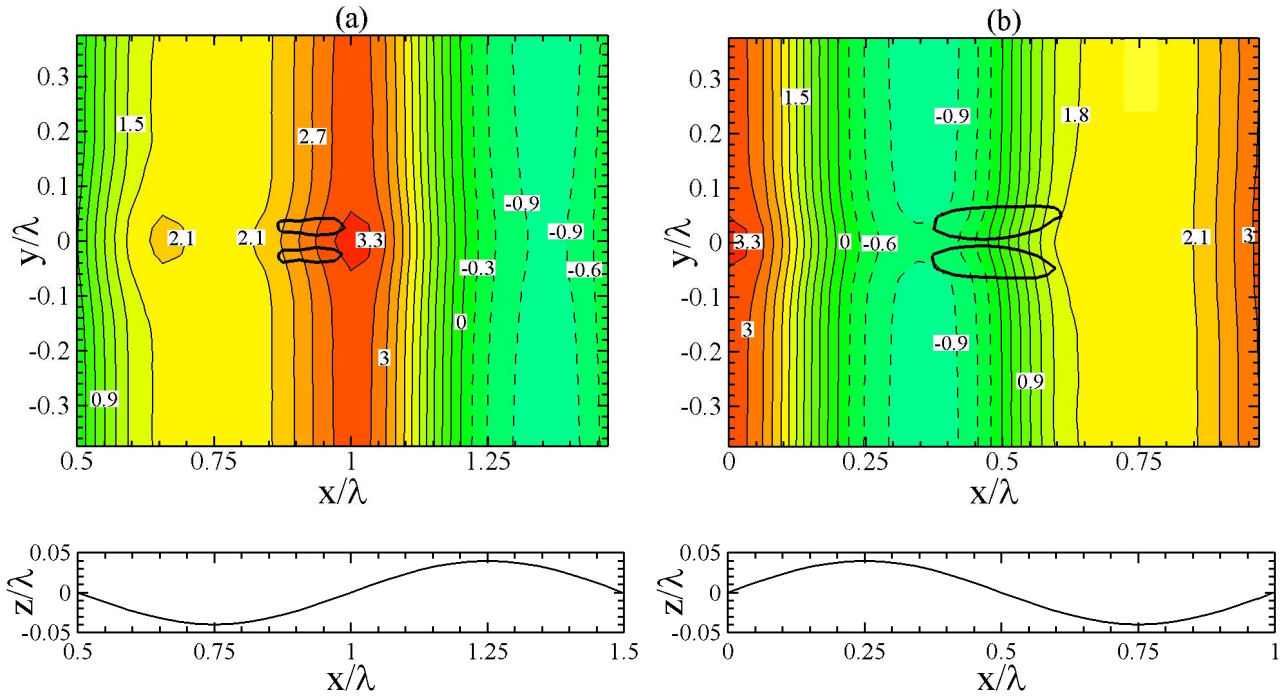

Figure 5. Conditionally-averaged surface shear stress contours above the water wave with steepness ak=0.25 and wave age c/u*=14. Samples are obtained by detecting: (a) Q1 (u'>0, w'>0) event above the windward face; and (b) Q4 (u'>0, w'<0) event above the leeward face. The locations of the vortical structures associated with the turbulent motions are denoted by thick solid lines. The bottom profile indicates the elevation of the surface wave.